9th International Workshop on the Physics of Compressible Turbulent Mixing
Cambridge, UK 19-23 July 2004 IWPCTM9

The problem of Kelvin-Helmholtz instability on contact boundary of finite width and ICF applications

Roman Stepanov[1], Angelo Caruso[2], Sergey Gus'kov[1], Vladislav Rozanov[1], Carmela Strangio[2], Nikolai Zmitrenko[3]

1. P.N. Lebedev Physical Institute of RAS, Moscow, Russia. romans@sci.lebedev.ru

2. ICF Physics and Technology Laboratory of C.R. ENEA, Frascati, Italy

3. Institute of Mathematical Modelling of RAS, Moscow, Russia

The research is partly supported by ISTC Project #1481

Topics

- Basic statement for KHI problem in Fast Ignition environment;
- Microscopic (uniform) fuel contamination: the source and effect on ignition conditions;
- Macroscopic contamination: simple estimations;
- DNS simulations of test problems;
- Conclusions

Basic paper is: A. Caruso, C. Strangio, JETP, 124, 5(11) 1058-1068 (2003).

Fast Ignition design

The so-called cone-focused fast ignition (CFFI, see S Hatchett et al., in *Proc. of 43rd Meeting Division of Plasma Physics*, APS (2001)) is one of the promising target design for inertial confinement fusion. In the CFFI a shell containing a layer of DT fuel is imploded by soft X-rays or laser light induced ablation, sliding along the external surface of a cone made of a high-Z material (see Fig. 1a). As a result of the implosion, a blob of compressed fuel is formed near the cone tip (see Fig. 1b). At this time, a short laser pulse is focused inside the cone to produce a forward jet of fast electrons. Passing through the cone material, the electrons can create an ignition spark on the compressed fuel assembly located nearby. Light ions (e.g. protons) also can be used as an energy vector.

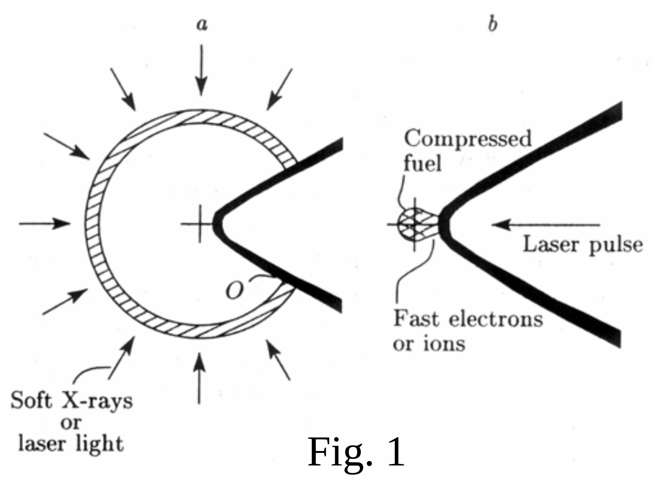

Fig. 1

High-Z contamination was found in experiments performed in the indirect drive mode. Vaporization of the cone material (gold) by X-rays passing through the imploding shell was indicated as responsible for this effect (see R.B. Stephens et al., Preprint GA-A24140 (2002)). Such a source of contamination should be absent in the direct-drive mode. But another source, potentially also active in this case, can be excited by the onset of the Kelvin-Helmholtz instability between the imploding shell and the cone surface.

During the implosion, the pressure in the acceleration stage can range from 1 to 100 Mb on the shell and from 1000 to 2000 Mb within the shell material at the transit near the cone tip. Pressures of this order are also exerted on the interface between the shell and the cone material. At such values of pressure, the cohesion forces in the cone material can be neglected and the shell containment by the cone is inertial. A very sketchy representation can be used to infer some of the basic flow features just near the leading shell points sliding on the cone (represented by O in Fig. 1a). We consider a reference frame attached to O and assume a locally planar 2D flow pattern. In this frame, the cone material impinges from the left at the velocity $\vec{V}_0$ ($|\vec{V}_0|$ is the implosion speed, see Fig. 2a). Main features of the flow are an oblique shockwave (angle ϕ) deflecting the cone material velocity by angle χ, from $\vec{V}_0$ to $\vec{V}$ and a slip surface (s) between the cone and the shell materials represented by the pressure wave.

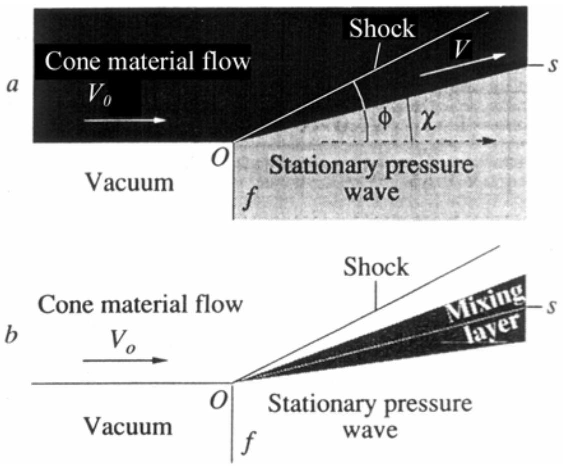

Fig. 2

Let us define the quantities $c_0 = \left(\frac{p}{\rho_s}\right)^{1/2}$, $\xi = \frac{\rho}{\rho_s}$, $M = \frac{V_0}{c_0}$, where ρ_s is the initial cone material (solid-state) density, p – pressure in the layer, ρ - density behind the shock. The relevant quantities for this study are V, χ, and ϕ given by

$$V = V_0\left(1 - \frac{1+1/\xi}{M^2}\right)^{1/2}, \ \sin\chi = \frac{1}{M}\left[\frac{\xi - M^2(\xi-1)}{1-\xi\left(M^2-1\right)}\right]^{1/2}, \ \sin\phi = \frac{1}{M}\left(\frac{\xi}{\xi-1}\right)^{1/2}$$

The above quantities are reported in Table 1 for regimes that can occur in the implosion of a thin spherical shell (e.g., with in-flight aspect ratio 14). The shell is first set on a low adiabat (ratio of the thermal electronic pressure to the Fermi pressure is 0.3) by a p_0=1 Mb pressure pulse (first shockwave). A gradual (adiabatic) rise of the pressure up to p=100p_0 then accelerates the shell to the maximum velocity. The shell material is finally left to freely implode towards the cone tip, where the pressure is expected to be 1000-2000 Mb.

Table 1

Reference case	p	V_0	ρ_{DT}	$c_{s\,DT}$	V	ρ_{Au}	$c_{s\,Au}$	χ	ϕ
First shockwave	1	6	0.78	1.7	≈6	26.2	0.42	1	7.5
End of accelerating pulse	100	15	10	4.3	14.8	76	1.6	7.6	10

The densities (ρ_{DT}, ρ_{Au}) and the sound velocities ($c_{s\,DT}, c_{s\,Au}$) were consistently estimated at the "real matter" level in the flowing cone material (gold) and for 0.3 adiabat in the "DT shell" set at rest. The units are Mb (pressure), g/cm^3 (densities), cm/µs (velocities), and degrees (angles). The effects of the shockwave on the gold flow appear relatively modest in the first two stages of the implosion. Severe flow distortion is produced near the cone tip.

Microscopic fuel poisoning

For any mechanism of contamination, it is not easy to evaluate the spectrum of sizes/masses of Au finally mixed into the compressed fuel as they undergo a complex evolution before being trapped in the ignition spark area. Two types of contamination can be expected, one in the form of mixing at the atomic level, the other as a distribution of Au blobs in the fuel. For small blobs, a two-step evolution can be expected. In the first, a gold blob immersed in a DT plasma at the temperature 10^8 K or higher and the density $\rho_{DT} = 200\,\mathrm{g/cm^3}$ is ablated by electronic thermal conduction and brought to the temperature and pressure equilibrium with the DT fuel. The second step is the diffusion of DT ions through the gold plasma. The diffusion length in a disassembling time is given by $R_{crit} = \sqrt{k_{DT} R_s / c_s}$, where k_{DT} is the diffusion coefficient of the average DT ion through gold plasma, and R_{crit} represents the largest blob that can be diffused through during the spark lifetime. The mass corresponding to this value can be estimated as $5 \cdot 10^{-13}$ g for $\rho_{Au} \approx 435\,\mathrm{g/cm^3}$ with $R_{crit} \approx 0.1\,\mu\mathrm{m}$.

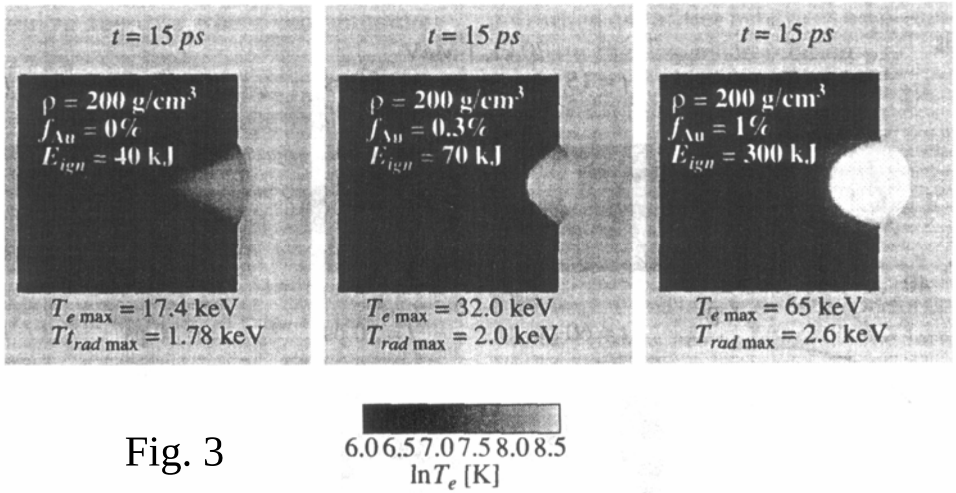

Fig. 3

Let us define the numeric fractions: $f_{Au} = \dfrac{n_{Au}}{n_{Au} + n_D + n_T}$, $f_D = f_T$, $f_D + f_T + f_{Au} = 1$ for gold, deuterium and tritium respectively. The beam of 1 MeV protons was used as driver, and f_{Au} was increased from 0.001% to 1.5%. The introduction of high-Z contamination affects the ignition through several mechanisms. Some of these are detectable through the inspection of Fig. 3. The electron temperature maps are given at the end of the igniting pulse for different degrees of doping. It can be seen that by increasing f_{Au}, the needed electron temperature increases. At the largest doping, the spark is imbedded in a thick radiation wave. The presence of gold affects the heat capacity and through this the igniting beam penetration depth, which is a self-consistent feature. The spiked structure disappears. The simulations show that due to the reduced DT content (about 57%) and to a smaller fractional fuel burn-up (about 25% instead of 38% of the clean fuel), the yield is decreased to about 40% that of the clean fuel case. It is to note, that in real situation the contamination of spark region is unlikely to be uniform, so the additional analysis is needed.

The results of the investigation for $f_{Au} \neq 0$ are shown in Fig. 4, where the data for the assigned density or pressure are shown. The two fitting curves are similar (exponential functions), with the one for a constant pressure (circles) being somewhat shifted to the right. In both cases, E_{ign} presents a steep increase as f_{Au} approaches 0.2% (about 14% by mass).

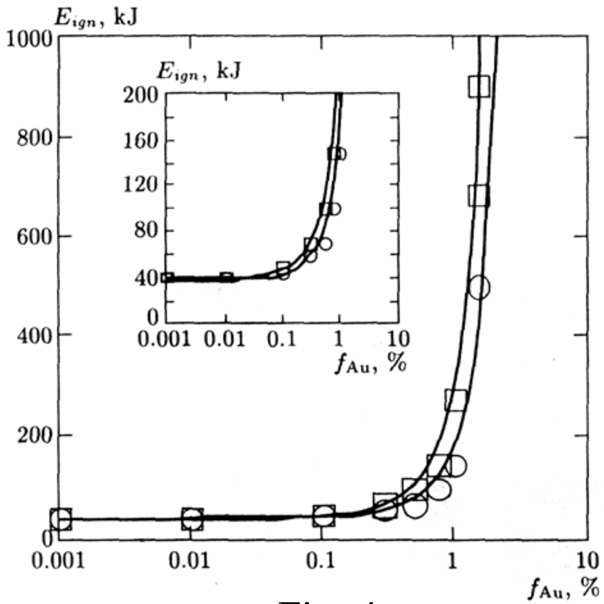

Fig. 4

Effects of macroscopic contamination

With regard to the effects of microscopic mixing, we estimate the typical size of the blobs that have a substantial effect on the ignition thresholds. Assuming the surface of a contaminant blob to be a sink for the fuel energy through the electron thermal flow, we can estimate the order of magnitude of the power W_a absorbed in the ignition spark by the contaminant as $W_a \approx \kappa_e T_e^{7/2} 4\pi \sum R_b$. Here κ_e is the Spitzer thermal conductivity coefficient and $\sum R_b$ is the sum of the blob radii contained in the spark. The total energy absorbed before spark disassembling is $E_a \approx W_a \left(R_s / c_{s\,DT} \right)$; this value has to be compared with the spark thermal energy E_{th}. For a standard spark ($T \approx$ 10 keV, $\rho_{DT} R_s \approx 0.5 \,\mathrm{g/cm^2}$), we find that $\dfrac{E_a}{E_{th}} \approx \dfrac{3.8 \sum R_b}{R_s}$. Setting this ratio to 0.5 implies that $\sum R_b \approx 0.13 R_s$. The "large-scale" blobs can be produced by the development of Kelvin-Helmholtz instability.

In the reference cases of Table 1, a treatment of KHI for compressible fluids with a discontinuous density and velocity of sound is required. The adopted geometry is shown on Fig. 5. The plane *xy* is taken on the slip surface *s* and the wave vector is taken in the plane xz. The flow is assumed at rest for $z<0$, in the region occupied by the imploding shell material. In the $z>0$ region, where the cone material flows, the velocity is set to the velocity V resulting from the shock analysis. Using linear approach (this assumption is yet to be proved because for supersonic motion perturbations may appear not to be small, and DNS results hold some evidences of it) and assuming that the perturbations behave as $\exp[-i\omega t + i(k_x x + k_z z)]$, we write the dispersion relation $c^2 r^2 \left(v^2 \omega^2 - 4 \right) (\omega - 2)^4 - \left[v^2 (\omega - 2)^2 - 4c^2 \right] = 0$, where $r = \dfrac{\rho_{Au}}{\rho_{DT}}$, $c = \dfrac{c_{s\,Au}}{c_{s\,DT}}$, $v = \dfrac{V \cos\psi}{c_{s\,DT}}$, and the complex frequency ω is normalized by $k_x V \cos\psi / 2$.

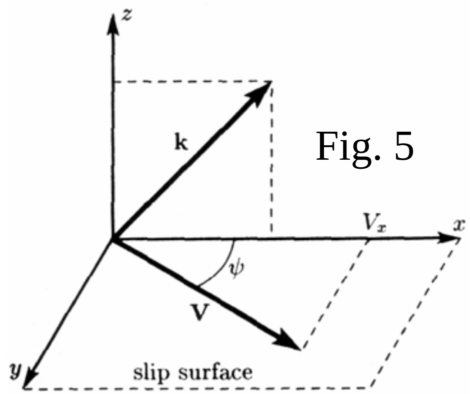

Fig. 5

The results are as follows. The interface is always unstable for waves with $90° \le \psi \le \psi_2$, where $\psi_2 \ge 0$. In this interval, the growth rate γ (the imaginary part of ω) starts from 0 at ψ=90°, achieves a maximum γ_m at some ψ_m, and vanishes again for $\psi=\psi_2$ if $\psi_2>0$. Furthermore, unstable modes can be found when $\gamma \ne 0$ for $\psi_2=0$. The results obtained in the reference cases are presented in Table 2, where angles are expressed in degrees, $\gamma_0 = \dfrac{\gamma_m}{k_x c_{s\,DT}}$, $\tau = \dfrac{\Delta}{\gamma_m t_{transit} \lambda_x}$; here Δ is the shell thickness, $t_{transit} = \Delta / V_0$, and $\lambda_x = 2\pi / k_x$. When $\tau(\lambda_x/\Delta) < 1$, the instability arises.

Table 2

Reference case	ψ_m	ψ_2	γ_m	τ
First shockwave	86	70	0.046	10
End of accelerating pulse	82	73	0.11	5

To roughly estimate the potential effect, let us assume that $h^2 \sim D(x/V)$, $D = a\gamma_m h^2$, where h is half-width of mixing layer at the distance x from O along $\vec{V}$ (see Fig. 2b), γ_m is evaluated for a typical wavenumber $k_x \approx h^{-1}$, and a is a suitable number. Because $\gamma_m \propto h^{-1}$, we find that $h \propto x$. For $a \approx 0.2$ this simple model applied to incompressible flows agrees satisfactorily with the experiment (see H. Schlichting, *Boundary Layer Theory*, McGraw-Hill (1968)). In the cases considered here the angle $\theta_{mix} = 2h/x$ is $\theta_{mix} = 2a\gamma_0 c_{s\,DT}/V$. The maximum thickness of the mixing layer is $\delta_{mix} \approx \theta_{mix}\Delta$; in the previously assumed reference situations, the results, ordered for increasing pressure, are $\theta_{mix} \approx$ 5, 10 and 70 mrad, and hence, for Δ = 100 μm, we have δ_{mix} = 0.5, 1, and 7 μm. It seems that the KHI, which is active during the shell implosion, is especially effective in the "near tip" region, where a substantial amount of matter can be collected and mixed into the fuel. Indeed, typically, the fuel masses of interest in CFFI (M_f) are of the order 3 mg at a density about 200 g/cm^3. The typical spark masses (M_{spark}) are of the order 3 μg. These masses should be compared with M_{Au} involved in the mixing. Estimating $M_{Au} = 0.5 f \rho_{Au} (\pi \sin\theta L^2 \delta_{mix})$, where θ = 30° is the cone half aperture, L = 400 μm is "sliding length", and assuming f = 0.3 to be the fraction of gold admixture entrained to the fuel, we obtain that $M_{Au} \approx$ 30 μg or $M_{Au} \approx 10 M_{spark}$. In the ignition study, it was found that a 14% mass admixture was sufficient to make ignition impossible.

DNS results

Linear analysis may appear not to be correct for the "near tip" regime of implosion. Thus, using NUT code we have performed series of direct numerical simulations for 2D planar geometry with different sets of parameters relevant for our reference case.

Statement of test problems

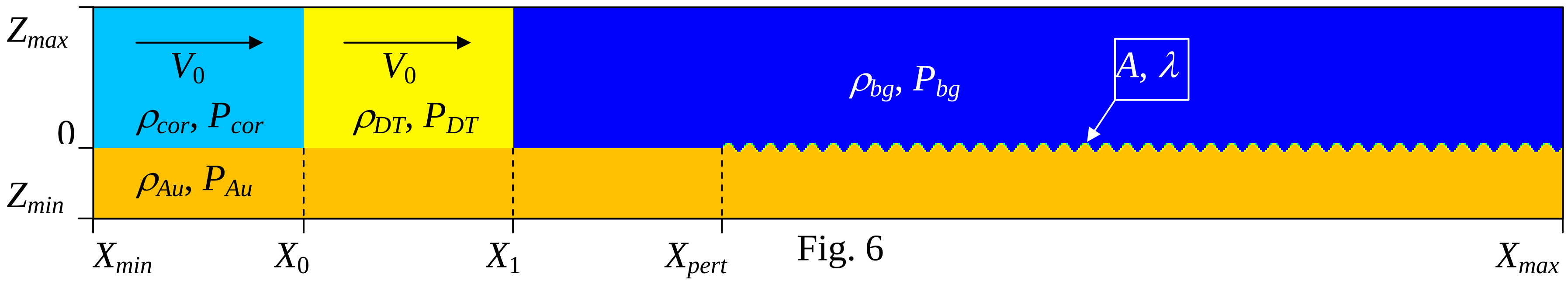

Fig. 6

Figure 3 represents main initial parameters for the simulations (note on units: [L]=mm, [t]=μs, [m]=mg):

ρ_{cor}, P_{cor} – density and pressure in the "corona",

ρ_{Au}, P_{Au} – density and pressure in the gold cone,

ρ_{DT}, P_{DT} – density and pressure in the DT layer,

ρ_{bg}, P_{bg} – density and pressure in the background gas,

A, λ - "amplitude" and "wavelength" of a perturbation (shape of perturbation vary between variants, see below),

V_0 – velocity of sliding of DT layer.

Meaning of other parameters is obvious. Frame boundaries were set to be free, thus providing fluid to flow freely through them.

There are several parameters, whose magnitudes were same for all variants: X_{min}=0; X_{max}=0.42; Z_{min}=-0.01; Z_{max}=0.02; $\Delta x=5\cdot10^{-4}$ (horizontal size of a cell); $\Delta z=2.5\cdot10^{-4}$ (vertical size of a cell); X_{pert}=0.18; X_1=0.12; $P_{cor}=P_{DT}=10^4$; $\rho_{cor}=10^{-2}$;

ρ_{DT}=10; ρ_{Au}=19.3; $\rho_{bg}=10^{-3}$; A=$6\cdot10^{-4}$; $\lambda=6\cdot10^{-3}$. Time step for simulations was being changed to satisfy Curant condition at every iteration, while outputs of data were separated by 0.04 ns ($4\cdot10^{-5}$ in time units of NUT)

All media were assumed to have ideal gas EOS with γ=5/3.

Other parameters for different variants are as follows:

ThickSine ("thick" DT layer and regular perturbations)

$P_{Au}=P_{bg}=10^{-1}$; V_0=150; X_0=0.06; shape of the perturbation is $z(x)=A\sin(2\pi(x-X_{pert})/\lambda)$;

ThickSineEngraved ("thick" DT layer and regular perturbations "engraved" into the cone)

$P_{Au}=P_{bg}=10^{-1}$; V_0=150; X_0=0.06; shape of the perturbation is $z(x)=A(\cos(2\pi(x-X_{pert})/\lambda)-1)$;

ThickSineEqualPressure ("thick" DT layer and regular perturbations, while initial pressure is uniform within the frame)

$P_{Au}=P_{bg}=10^{4}$; V_0=150; X_0=0.06; shape of the perturbation is $z(x)=A\sin(2\pi(x-X_{pert})/\lambda)$;

ThickSineLowMach ("thick" DT layer and regular perturbations, while the speed of DT layer and "corona" sliding was set to be subsonic related to the DT)

$P_{Au}=P_{bg}=10^{-1}$; V_0=30; X_0=0.06; shape of the perturbation is $z(x)=A\sin(2\pi(x-X_{pert})/\lambda)$;

ThinSine ("thin" DT layer and regular perturbations)

$P_{Au}=P_{bg}=10^{-1}$; V_0=150; X_0=0.108; shape of the perturbation is $z(x)=A\sin(2\pi(x-X_{pert})/\lambda)$;

ThickRandom ("thick" DT layer and random perturbations)

$P_{Au}=P_{bg}=10^{-1}$; V_0=150; X_0=0.06; shape of the perturbation is set to be an array of "bumps" with amplitude *ampl* and width *scale* to be defined as:

$ampl=s\cdot A\cdot\min(z_r,2)$; $scale=0.5\cdot A\cdot\lambda/(|ampl|+A)$, where z_r is random value, normally distributed with zero mean and unit standard deviation, which was independently generated for each "bump", and $s=\mathrm{sign}(z_r)$.

Brief description of results

Due to lack of place we will briefly consider only **ThickSine** variant (complete series can be viewed via notebook)

This variant holds basic information about the effect

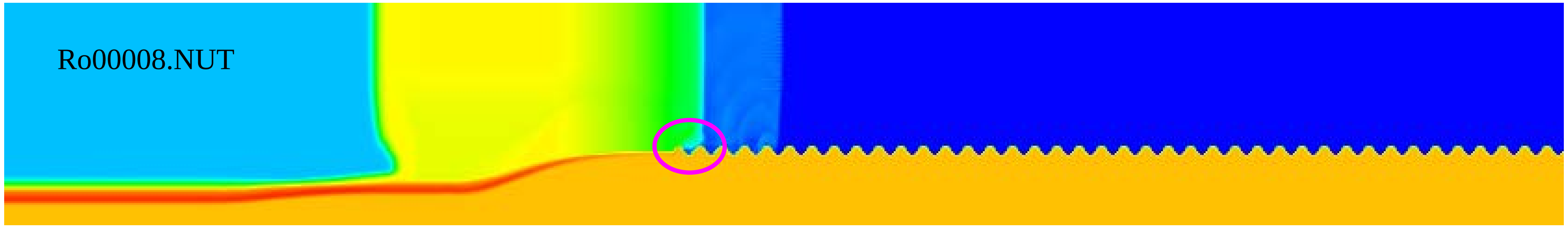

At this moment the formation of an "air cushion" can be observed.

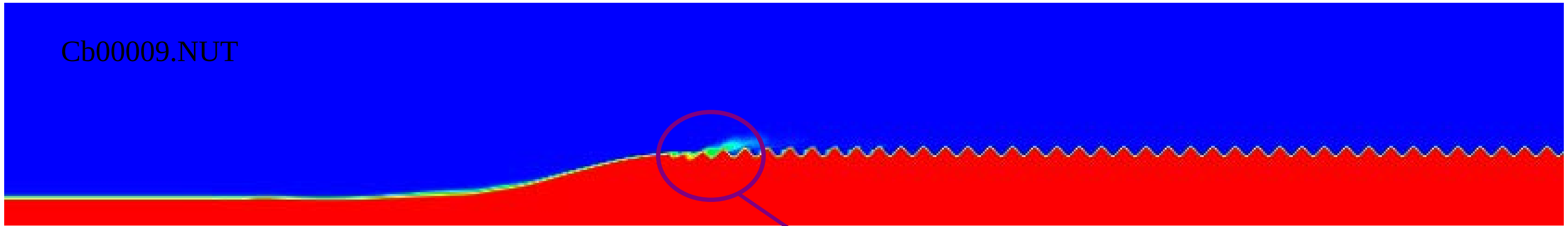

The above picture shows the formation of a "blob" of gold, which then will be transported by rarefaction wave front

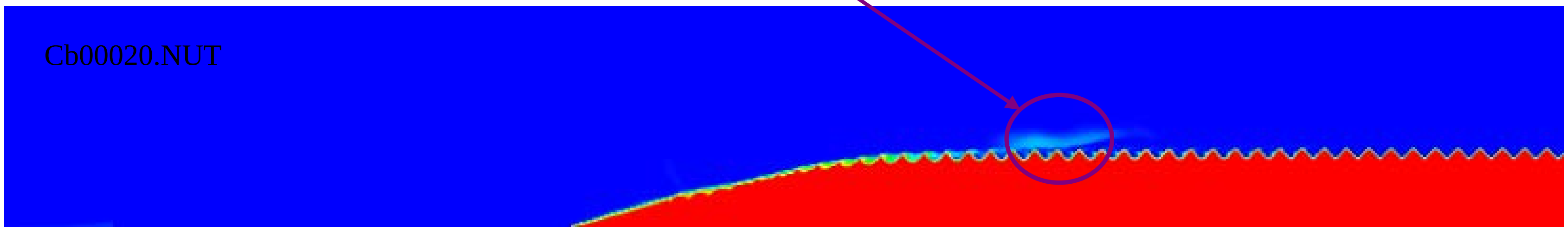

Investigating evolution of density field one may observe the formation and passage of shockwave through the cone and its interaction with perturbations:

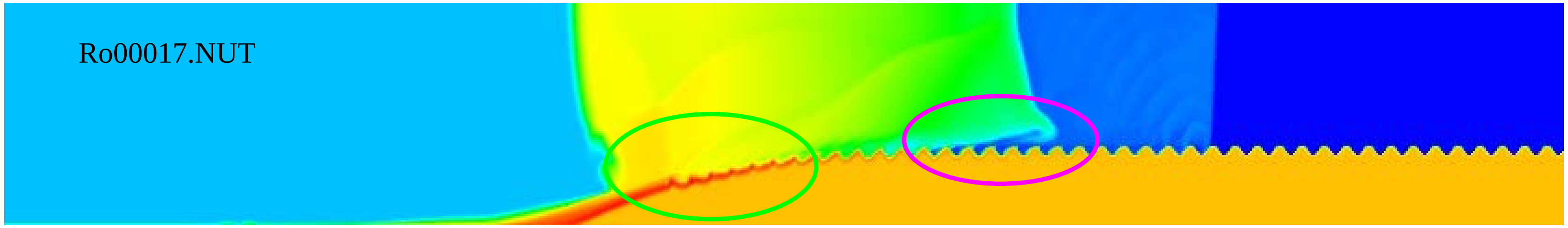

This is the evidence for Richtmyer-Meshkov instability (but of uncommon type, due to very special density/pressure/velocity arrangement at the interface) to play dominant role while the layer is passing along the boundary. It is to note, that for this variant the speed of sliding is supersonic, thus making linear approach to estimate Kelvin-Helmholtz effect to be scarcely applicable. The analysis rather should take into account the ratio between time of passage of a layer and characteristic time of development of shock process. The above picture also shows the “air cushion” effect in its dynamics. Next picture depicts the behavior of gold concentration at the same time moment:

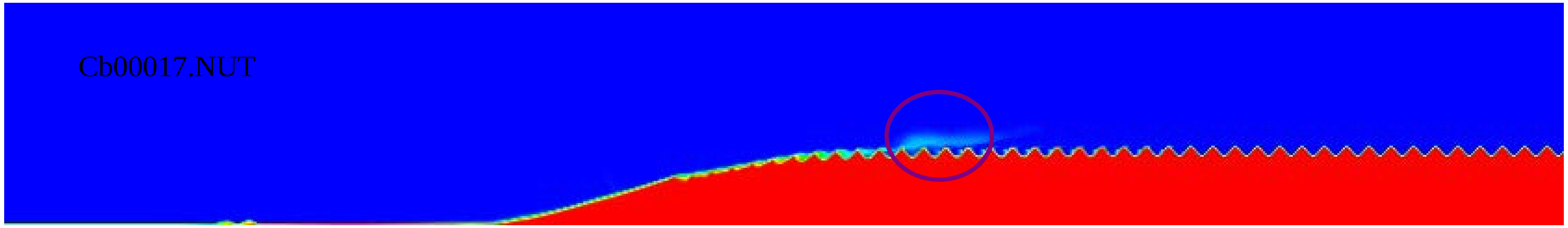

One can observe, that there is no sufficient admixture of gold into DT, with the exception for above mentioned “blob” formed at early stage of the process. It seems, that DT rarefaction produce pre-shock of gold, while in the rarefaction wave density is not high enough to produce KH-induced mixing. As a whole, the process resembles “a wind over dunes” picture with additional influence of shock-produced “driving in”.

The described qualitative physics remains sufficiently untouched for other variants, excepting **ThickSineEqualPressure**; this fact seems to prove above made statements: e.g. for the **ThickSineLowMach** variant the rarefaction wave which propagates into background gas, forms the same “quasi-RM” picture. Thus, let us briefly introduce some pictures of density and Au concentration fields for **ThickSineEqualPressure**:

Density (log scale)

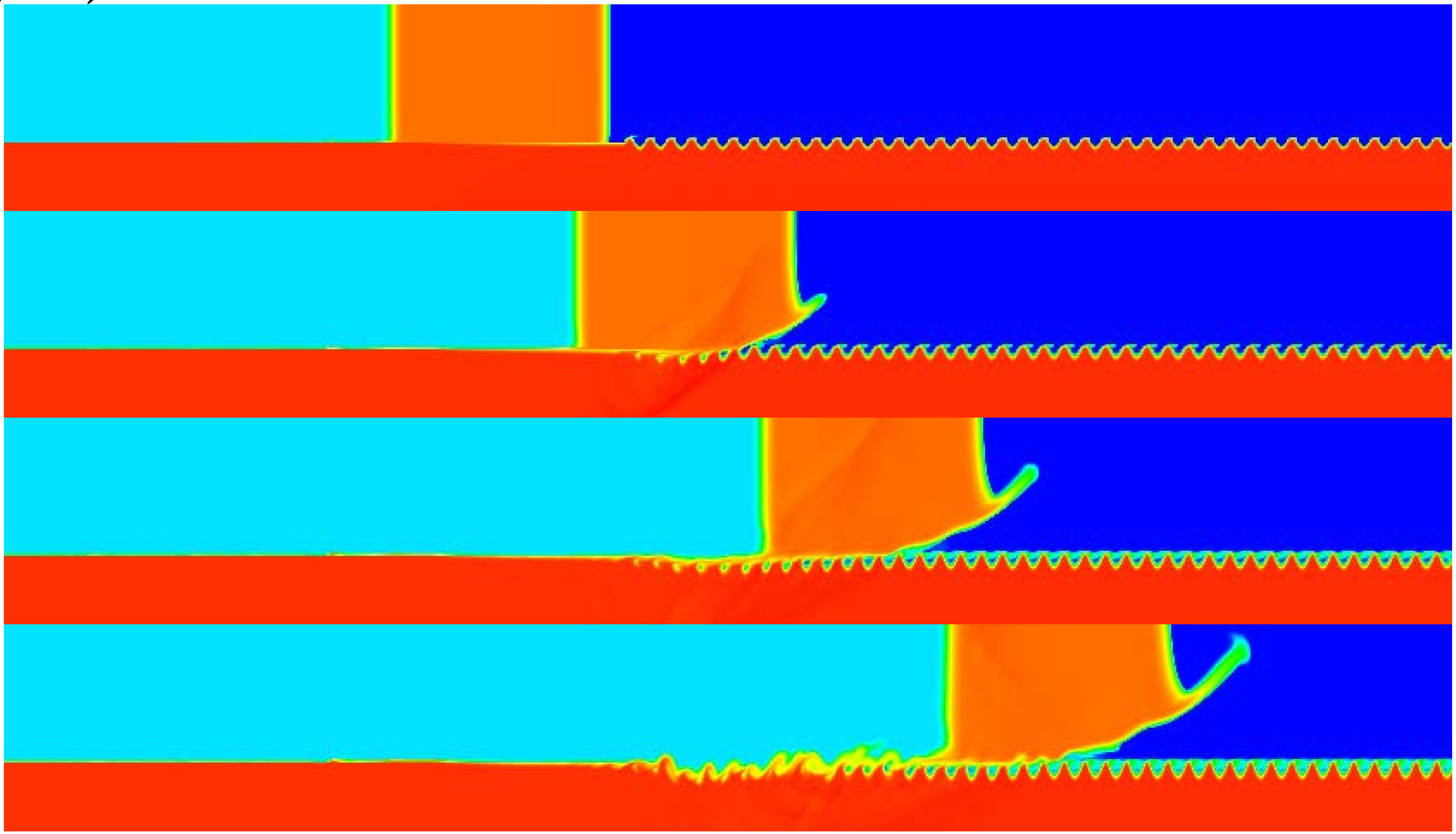

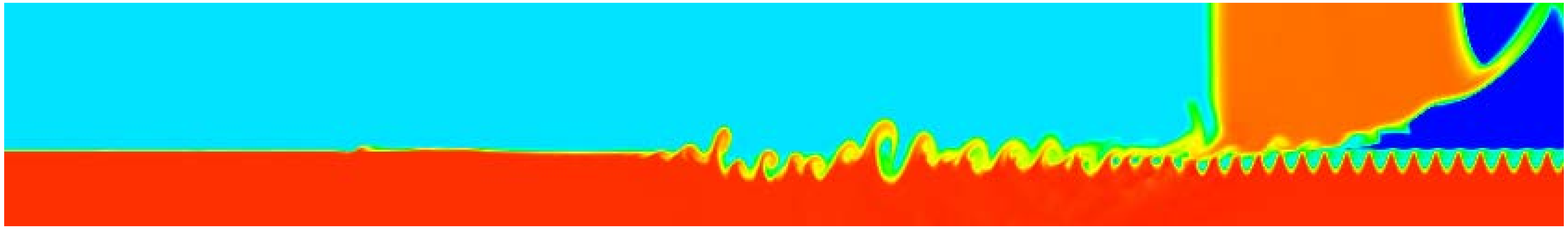

Au concentration (correspond for three latter density plots)

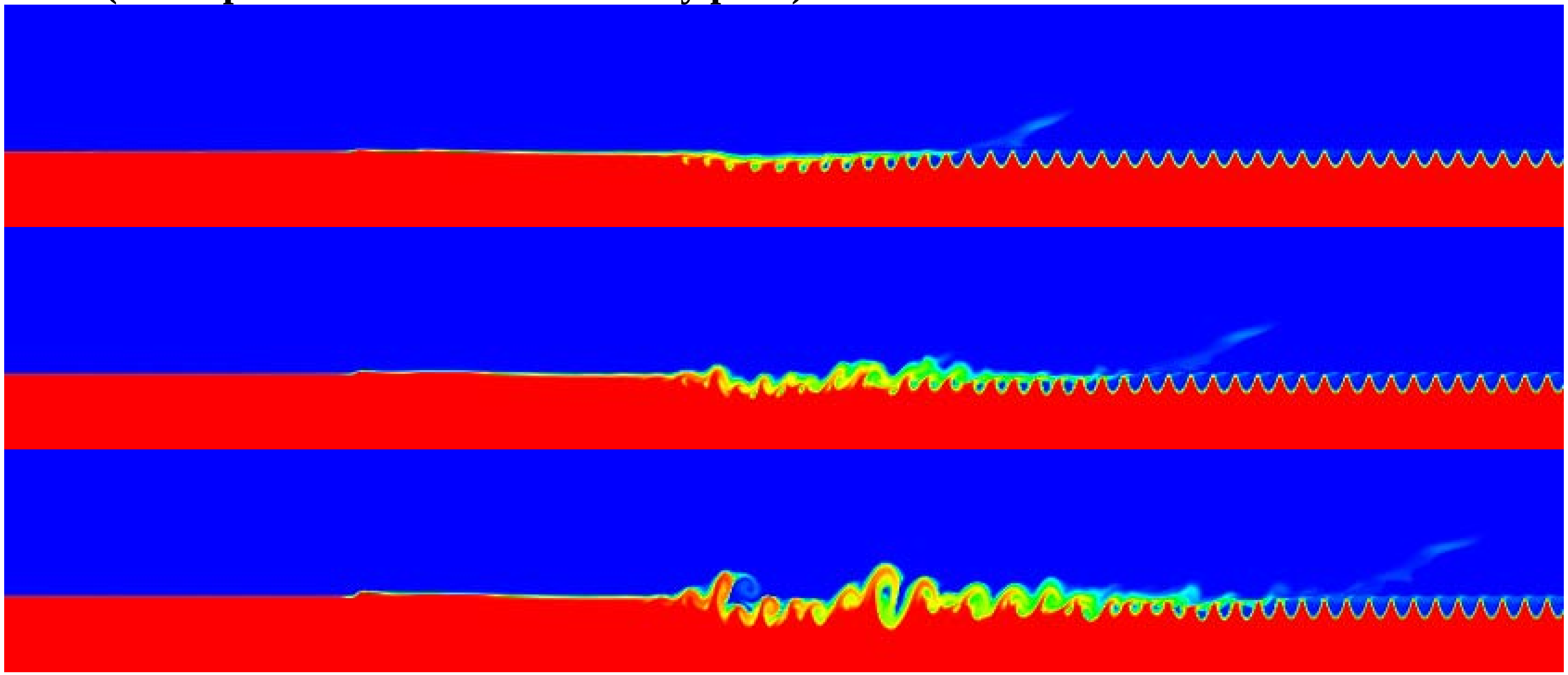

Despite the fact that Au admixture to fuel is still small (mixing develops after passing of the layer) it is clear that KH-process (nonlinear) is the leading one here. It is worth noting that very similar picture may be found while analyzing **ThinSine** variant, but the origin of gold-“corona” mixing seems to differ from the described one (see the figure below):

Ro00021.NUT

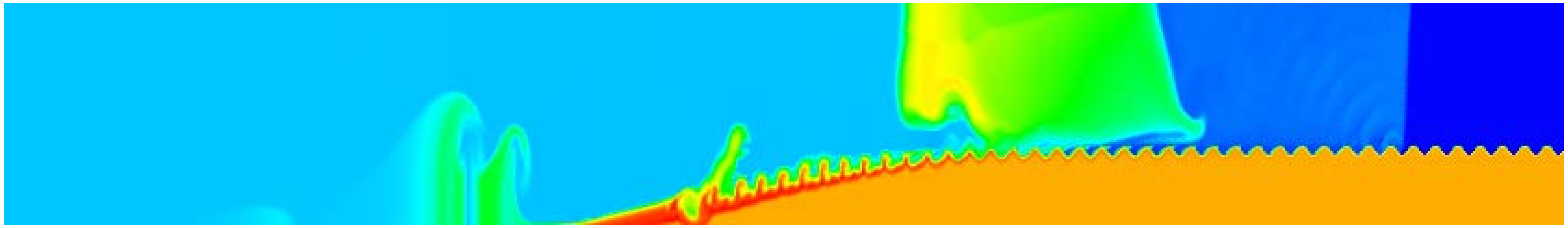

Cb00021.NUT

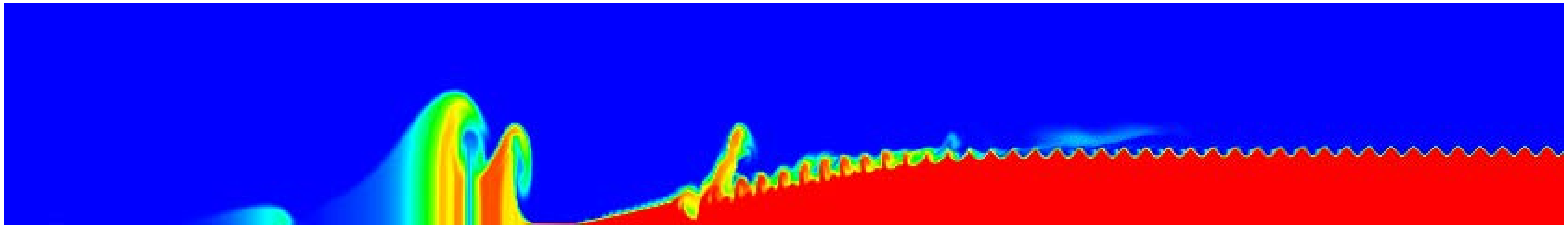

CMb00021.NUT

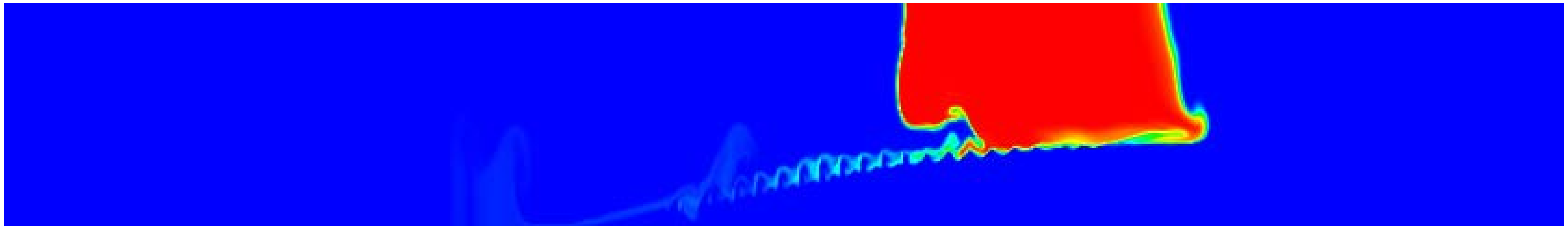

The DT-layer is rather pushed away of the cone, and the reason may be that, due to small thickness of layer, in the vicinity of DT-Au interface “superposition” of two rarefaction waves (into background gas and into the cone) leads to forming an area of decreased pressure in DT, and this area, in turn, provide “corona” gas to break through the layer.

Conclusions

The process of turbulent mixing of a layer of finite thickness with perturbed surface of a cone for typical Fast Ignition environment is very interesting phenomenon, but also very complex one. The "quasi-RM" instability may be of most significance, so the "governing" values to calculate are: the characteristic time of transition of generated shockwave through perturbed interface, the characteristic time of a perturbation dynamics after passing of the shockwave. Finally, these characteristic times should be compared with layer's "time of flight" Δ/V_0, where Δ is layer thickness and V_0 – layer speed, and with characteristic time of supersonic shear turbulence. Depending on these ratios there could be different regimes of evolution.

The applied problem considered in the paper gives rise to the following fundamental statement of problems related to hybrid RM-KH instability. First of them is the instability of a boundary between two semiinfinite liquids with large boundary pressure jump, slipping relatively each other. The feature peculiar to this configuration is initiation and propagation of the transient shockwave and its interaction with perturbations. Second, the configuration of finite thickness layer moving along semiinfinite substrate under the condition of pressures in both media to be equal. This statement will allow one to investigate the effect of layer thickness and slip velocity (sub- or supersonic) on instability evolution and mixing. Third statement incorporates the physics of the above two problems, namely, the evolution of perturbations at the boundary of finite layer slipping over a substrate, while pressure in layer is significantly higher then one in the substrate. The formation of oblique shock wave is specific to this statement. The dynamics of perturbations in latter two statements is governed, among other, by the parameter which is the ratio between perturbation amplitude/wavelength and layer thickness.